



## Electrochemical and Infrared Studies of the Reduction of Organic Carbonates

Xuerong Zhang,\* Robert Kostecki,\* Thomas J. Richardson,\* James K. Pugh, and Philip N. Ross, Jr.\*<sup>z</sup>

Lawrence Berkeley National Laboratory, University of California, Berkeley, California 94720, USA

The reduction potentials of five organic carbonates commonly employed in lithium battery electrolytes, ethylene carbonate (EC), propylene carbonate (PC), diethyl carbonate (DEC), dimethyl carbonate (DMC), and vinylene carbonate (VC) were determined by cyclic voltammetry using inert (Au or glassy carbon) electrodes in tetrahydrofuran/LiClO<sub>4</sub> supporting electrolyte. The reduction potentials for all five organic carbonates were above 1 V (vs. Li/Li<sup>+</sup>). PC reduction was observed to have a significant kinetic hindrance. The measured reduction potentials for EC, DEC, and PC were consistent with thermodynamic values calculated using density functional theory (DFT) assuming one-electron reduction to the radical anion. The experimental values for VC and DMC were, however, much more positive than the calculated values, which we attribute to different reaction pathways. The role of VC as an additive in a PC-based electrolyte was investigated using conventional constant-current cycling combined with *ex situ* infrared spectroscopy and *in situ* atomic force microscopy (AFM). We confirmed stable cycling of a commercial li-ion battery carbon anode in a PC-based electrolyte with 5 mol % VC added. The preferential reduction of VC and the solid electrolyte interphase layer formation therefrom appears to inhibit PC cointercalation and subsequent graphite exfoliation.  
 © 2001 The Electrochemical Society. [DOI: 10.1149/1.1415547] All rights reserved.

Manuscript submitted March 6, 2001; revised manuscript received July 13, 2001. This was Paper 136 presented at the Phoenix, Arizona, Meeting of the Society, October 22-27, 2000. Available electronically November 1, 2001.

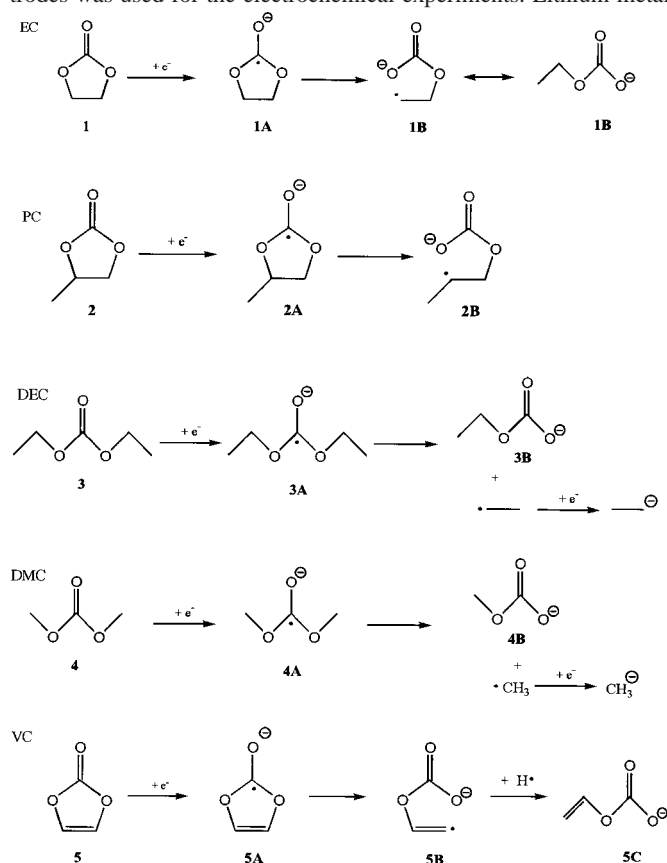
Electrolytes typically used in lithium batteries consist of a lithium salt dissolved in an organic solvent, or a mixture of these solvents. The solvents fall into two general classes: ethers or alkyl esters of carbonic acid. Because of lower volatility and higher flash point, the organic carbonates are the preferred solvent class in commercial batteries. Propylene carbonate (PC) has many advantages over other organic carbonates for use in the battery electrolyte, *e.g.*, lower cost and better low temperature performance. Use of PC in Li-ion batteries has, however, been problematic due to cointercalation of solvent molecules along with Li<sup>+</sup> ion into the graphite and subsequent exfoliation.<sup>1</sup> The electrolyte commonly used in commercial li-ion cells is based on ethylene carbonate (EC), even though these batteries have poorer low temperature performance.<sup>2</sup> Research efforts have, with some success,<sup>3,4</sup> pursued additives to PC to generate a solid electrolyte interphase (SEI) layer that prevents PC cointercalation. The mechanism of functioning of these additives is, however, still uncertain.

We have performed quantum chemical calculations of the thermodynamic reduction potential of eleven organic molecules at an inert electrode, assuming one-electron reduction to the radical anion as the first step.<sup>5</sup> The ethers in general were found to be much more stable to reduction than were the organic carbonates, and are not expected to be reduced before the deposition of lithium metal. The reduction potentials of organic carbonates were calculated to be positive to the lithium potential, with EC being the most positive, 1.46 V vs. Li/Li<sup>+</sup>. Here, we report our experimental determinations of the reduction potentials of EC, PC, diethyl carbonate (DEC), dimethyl carbonate (DMC), and vinylene carbonate (VC), and compare them with calculated values. The postulated reduction reactions for the five organic carbonates discussed here are shown in Scheme I. These mechanisms are in general agreement with those postulated in the literature, as discussed in greater detail elsewhere.<sup>5</sup> The role of VC as an additive was investigated also, and so was the SEI layer resulting from its reduction characterized by infrared spectroscopy.

### Experimental

Tetrahydrofuran (THF) (Aldrich, 99.9+%, HPLC grade), EC (Grant Chemical, less than 20 ppm H<sub>2</sub>O), LiClO<sub>4</sub> (EM Industries), DMC (Grant Chemical, less than 20 ppm H<sub>2</sub>O), DEC (Grant Chemical, less than 20 ppm H<sub>2</sub>O), PC (Grant Chemical, less than

20 ppm H<sub>2</sub>O), and VC (Aldrich, 97%) were used as received without further purification. A single compartment glass cell with three electrodes was used for the electrochemical experiments. Lithium metal



Scheme I.

was used for both counter and reference electrodes. The target solvent specie was dissolved in a THF/0.1 M LiClO<sub>4</sub> supporting electrolyte to a concentration typically of 1 vol % (5 mM in the case of EC). Three different working electrodes were used. A 1 mm radius Au millielectrode was used in cyclic voltammetry (CV) experiments. A glassy carbon (GC) electrode (1 × 1 cm) was used for the Fourier transform infrared (FTIR) experiments with VC. A commer-

\* Electrochemical Society Active Member.

<sup>z</sup> E-mail: PNRoss@lbl.gov

cial (PolyStor, Pleasanton, CA) Li-ion battery composite carbon electrode was used for the cycling. The composition of the anode was 75% mesocarbon microbead (MCMB) carbon, 17% SFG-6 graphite, and 8% polyvinylidene difluoride (Kureha C) with a loading of  $5.5 \text{ mg/cm}^2$  applied to both sides of a Cu foil current collector.

For the FTIR experiments, the GC electrode was cycled at  $20 \text{ mV/s}$  between  $0.1$  and  $2 \text{ V}$ , held at the VC reduction potential for  $5 \text{ min}$ , then brought back to  $2 \text{ V}$ . The electrode was emersed from the cell at  $2 \text{ V}$ , and inserted without rinsing into a gastight IR cell fitted with a KBr window. *Ex situ* IR microscopy was conducted using a Nicolet Magna 760 spectrometer fitted with a Nic-Plan IR Microscope.

*In situ* atomic force microscopy (AFM) images were obtained with a Molecular Imaging (MI) scanning probe microscope coupled with a Park Scientific Instruments (PSI) electronic controller. The electrochemical cell is composed of three electrodes, with GC being the working electrode and lithium foil being the reference and counter electrode. The AFM was used in the constant-force mode with PSI MLCT-AUNM (Park Instruments) microcantilevers ( $0.05 \text{ N m}^{-1}$ ) to determine the morphology of the carbon electrode surface. These measurements were conducted in a small glove box under helium atmosphere.

### Results and Discussion

**Reduction potentials.**—Solvent reduction potentials were determined by CV. The sweep rates were  $2\text{--}5 \text{ mV/s}$ . The solvent specie was dissolved in a THF/LiClO<sub>4</sub> supporting electrolyte to a concentration of *ca.*  $1 \text{ vol } \%$ . A low concentration was used to minimize the effect of impurities, *e.g.*, water and the inhibitor in VC, on the voltammetry. Due to diffusion-limited flux,<sup>6</sup> for concentrations less than  $10^{-4} \text{ M}$ , the total amount of material electrodeposited under a linear sweep voltammetry peak at  $2\text{--}5 \text{ mV/s}$  is less than one “monolayer” ( $<200 \text{ } \mu\text{C/cm}^2$ ). THF was selected because of its stability toward reduction above the lithium metal potential, as seen from the control scans (Fig. 1). The cathodic peak at  $1.6 \text{ V}$  is generally ascribed to the reduction of H<sub>2</sub>O or oxygen impurities in the electrolyte.<sup>7</sup> We agree with Aurbach *et al.*<sup>7</sup> that the coupled peaks at around  $0.6 \text{ V}$  (cathodic) and  $0.9 \text{ V}$  (anodic) correspond to underpotential deposition (UPD) and anodic stripping, respectively, of lithium metal on the gold surface. These peaks do not appear when a tetrabutylammonium cation is used in the electrolyte in place of a lithium ion. The UPD of Li from ethereal solvent is more complex than for other metals in aqueous electrolyte and is a phenomenon beyond the scope of the present work. The interested reader should consult the more detailed study by Aurbach *et al.*<sup>7</sup>

Characteristic voltammetry curves for the organic carbonates are shown in Fig. 1 and the reduction potentials are summarized in Table I. The experimental values for EC, DEC, and PC are in reasonable agreement with the calculated values, while those for DMC and VC are significantly lower. For EC and PC, the calculation assumes one-electron transfer to form the bond broken form of radical anion (see Scheme). The reduction of the two linear carbonate solvents (DEC and DMC) was assumed<sup>5</sup> to have another one-electron transfer to the alkyl radical that was broken off from the radical anion generated initially, forming an alkyl anion. The first electron transfer breaks the C-O bond forming an alkyl carbonate anion and an alkyl radical, and the second electron transfer is to the alkyl radical to form an alkyl anion (see Scheme I). The reduction potential calculated based on this assumption is in good agreement with the experimental values for DEC, but not for DMC. It is energetically unfavorable for a methyl radical to accept an electron to form a methyl anion, which consequently lowers the calculated reduction potential for DMC *vs.* that for DEC. This implies that the reduction of DMC follows a different reaction pathway. The reduction potential of VC was calculated with 5A rather than 5B being the final product due to instability of the vinyl radical in 5B. The high experimental reduction potential obtained for VC implies a different reaction pathway for this molecule as well.

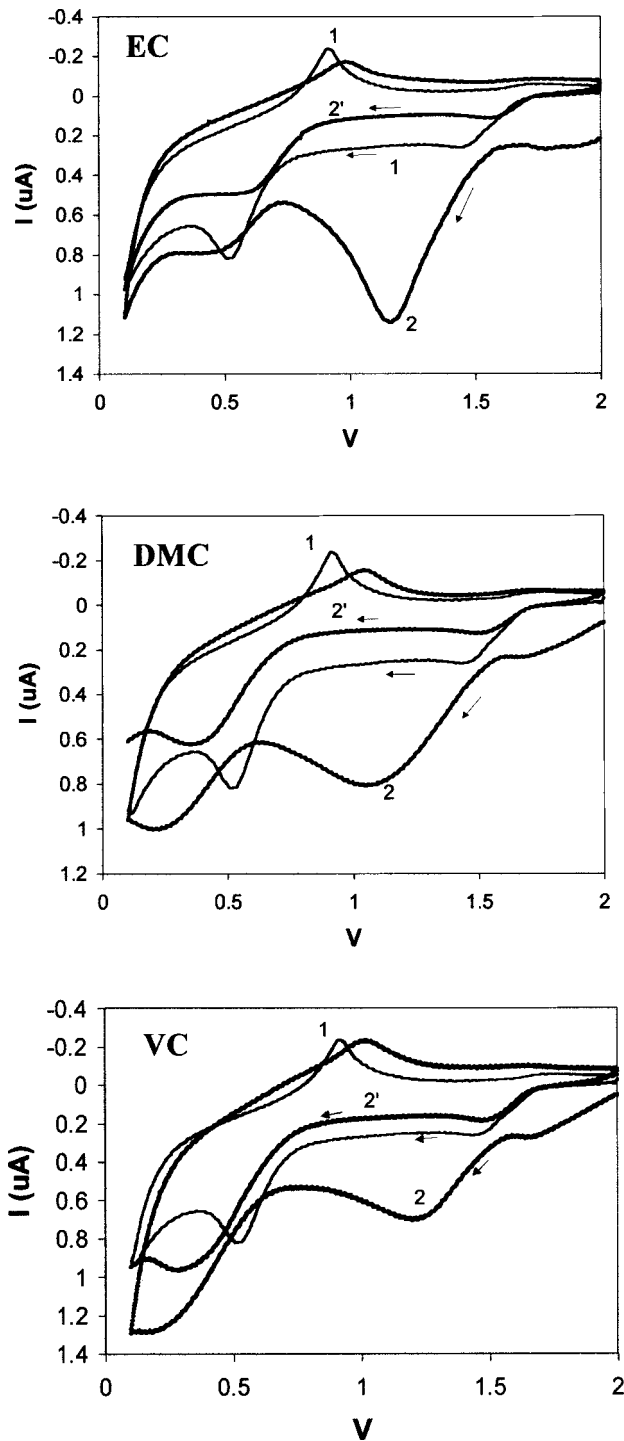


**Figure 1.** CV for THF-based electrolyte (1) without target solvent species and with solvent species, (2) for the first cycle and (2') for the second cycle. Only the negative-going potential sweep is shown for the second cycle.

EC was the only solvent that produced a single reduction peak on the first cathodic sweep, the others having some ill-defined cathodic process(es) below  $0.5 \text{ V}$ . The product formed by the initial reduction of EC appears to be more stable than that formed by reduction of the other carbonates. It is also the only carbonate in which Li UPD is clearly seen, as in the supporting THF electrolyte, indicating the reduction product of EC does form a functioning SEI layer on Au. This chemistry is consistent with the general acceptance of EC-based electrolyte in li-ion batteries.

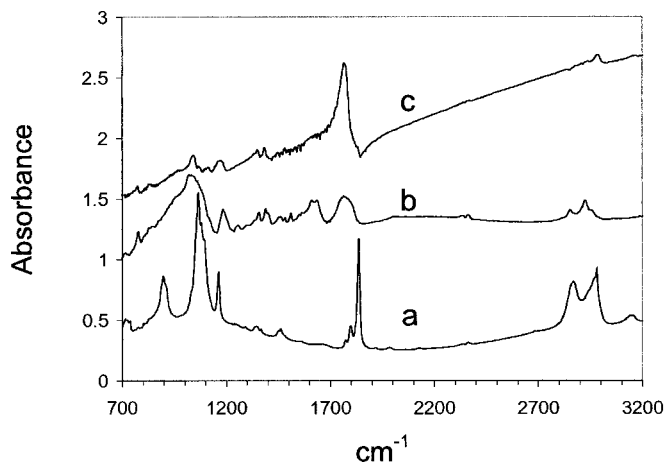
**Table I. Comparison of calculated<sup>5</sup> and experimental potential values of solvent reduction.**

Solvent	Calculated	Experimental
EC	1.46	1.36
DEC	1.33	1.32
PC	1.24	1.00-1.60
DMC	0.86	1.32
VC	0.25	1.40

The CV of PC reduction has (not shown) a shallow and broad feature ranging from 1.6 to 1 V, most probably indicating slow reduction kinetics. This is consistent with most of the literature reports on PC reduction. Aurbach *et al.* also did not observe a clearly resolved feature for PC reduction on Au, only a large cathodic background current that was ascribed to the solvent reduction. While a definite reduction potential could not be established, their concurrent FTIR results indicated that PC reduction occurred at a potential as high as 1.5 V. Campbell<sup>8</sup> reported a similar result in neat PC with a Pt microelectrode: a broad cathodic wave beginning at 1 V. The use of neat solvent eliminated the possibility of salt reduction, and the cathodic process beginning at *ca.* 1 V was assigned to the reduction of PC. The same group also reported that the presence of water or 1,2-propanediol in PC enhanced the cathodic current. Pletcher *et al.*<sup>9</sup> observed similar cathodic currents in PC-based electrolyte with a Ni electrode. They argued, however, that the observed magnitude of the cathodic current was too small for solvent reduction at such a high concentration of PC and therefore, could not be ascribed to its reduction. They proposed that it was more likely the reduction of trace water. The PC concentration in the THF supporting electrolyte in our experiments was 1 vol %. The amount of water introduced by PC addition, therefore, would be very small. The observed reduction in electrolyte with PC, which was not seen in the supporting THF electrolyte, should indeed be reduction of the PC solvent. The slow kinetics makes it impossible to assign a definite value to the reduction potential, it lies somewhere in the range of 1-1.6 V. The calculated value of 1.24 V is within this range. The PC slow reduction kinetics is consistent with the hypothesis<sup>1</sup> that PC is cointercalated first with Li<sup>+</sup> into graphite and subsequently reduced causing exfoliation of the electrode.

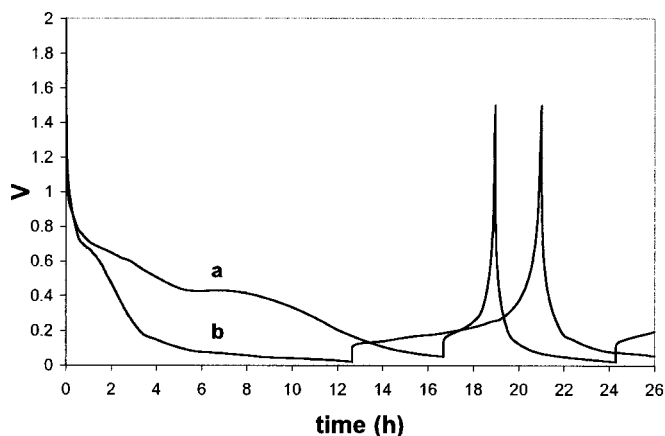
The relatively positive reduction potential for VC supports one of the postulated mechanisms of action of VC as an additive to PC-based electrolyte for Li-ion cells. Similar to EC, preferential reduction of VC could form an interfacial layer that prevents PC cointercalation and graphite exfoliation.

**Infrared reflection absorption spectroscopy (IRRAS).**—VC is reduced at 1.40 V, much higher than the calculated value of 0.25 V, which suggests that one-electron transfer that the unsaturated radical anion (5A in Scheme I) is not a stable intermediate as was assumed in the calculation.<sup>5</sup> Rather, a more energetically favorable intermediate is formed. IRRAS was used to investigate the chemistry of VC reduction, and to identify what this intermediate might be. The results (Fig. 2) indicate that the VC molecule is reduced to unsaturated alkylcarbonate anion. IRRAS spectra from the surface of the GC electrode held at 1.2 V in THF supporting electrolyte with 5 vol % VC shows new peaks different from the supporting electrolyte, and attributed to VC reduction. The absorption peak at 1640 cm<sup>-1</sup> corresponds to the C=O stretching mode of an alkyl carbonate, and 1620 cm<sup>-1</sup> is assigned to the C=C double bond stretching mode. Note that the C=C double bond stretch is missing in the spectrum of the electrolyte before reduction due to the symmetry of the VC molecule, *i.e.*, the C=C double bond stretch in VC is IR-inactive.<sup>10</sup> Its appearance in the IR spectra after reduction suggests a ring opening of VC, which creates an unsymmetrical environment about the C=C bond, and causes it to be IR-active. The broad shoulder at 980 cm<sup>-1</sup> is assigned to the out-of-plane C-H bending mode of a methylene (=CH<sub>2</sub>) group.<sup>10</sup> All of these point to lithium vinyl carbonate

**Figure 2.** IRRAS of (a) VC/THF-LiClO<sub>4</sub> electrolyte before reduction, (b) VC/THF-LiClO<sub>4</sub> electrolyte after reduction, and (c) GC electrode surface after reduction in VC/THF-LiClO<sub>4</sub>.

as one of the reduction products of VC, and a major component in the organic layer of the SEI. The suggested reduction mechanism of VC, shown in Scheme I, involves the formation of a bond broken radical anion (5B), which undergoes a hydrogen abstraction to produce the unsaturated alkylcarbonate anion (5C). We have, however, not yet calculated the reduction potential for this reaction pathway. The spectrum for the bulk electrolyte after reduction shows similar features to that from the electrode, which suggests that the lithium vinyl carbonate salt is partly soluble in the electrolyte.

**SEI formation by VC reduction.**—Figure 3a shows constant-current (0.5 mA/cm<sup>2</sup>) cycling of the composite carbon anode in PC electrolyte with 1 M LiClO<sub>4</sub>. The long plateau around 0.4 V indicates significant solvent reduction. In consequence, the reversible capacity for the first cycle was only 12%. Severe graphite exfoliation was observed in this electrolyte after just 10 cycles, and concurrent loss of capacity. Figure 3b shows the first constant-current charge and discharge of a nominally identical composite carbon anode in the same PC with addition of 5 vol % VC. The reversible capacity on the first cycle is significantly improved to 67%, and subsequent cycles had a cycling efficiency of 93-95%. The electrolyte turned slightly brown after 10 cycles. There was, however, no observable exfoliation of the graphite. The effects of VC on PC reduction reported here are qualitatively consistent with those re-

**Figure 3.** Constant-current (0.5 mA/cm<sup>2</sup>) cycling of a composite carbon anode in (a) PC/LiClO<sub>4</sub> electrolyte, (b) PC/LiClO<sub>4</sub> electrolyte with 5% VC added.



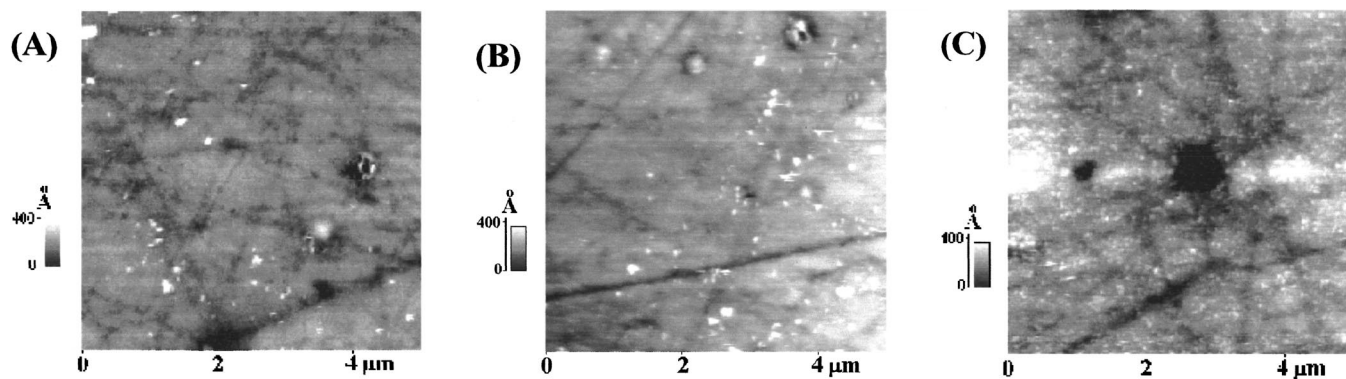


Figure 4. AFM image of a GC electrode surface at (A) OCP 2.0 V, (B) 1.2 V, and (C) 0.8 V.

ported previously by Jehoulet *et al.*<sup>4</sup> This group focused on gas production during the formation charge, and demonstrated that the amount of gas produced in a PC/EC/DMC mixed solvent decreased significantly when 5% VC was added. This was attributed to a suppression of solvent decomposition. The same group also reported that the electrochemical reduction of VC did not release gaseous product.

The effects of VC on the cycling of a graphite electrode in PC electrolyte suggests that VC reduction takes place at potentials above 1.2 V, before  $\text{Li}^+$  ion intercalation, and forms a protective layer that prevents PC cointercalation and graphite exfoliation. Although the other carbonates EC, DEC, and DMC also have reduction potentials positive of  $\text{Li}^+$  ion intercalation, use of EC/DEC/DMC as additives to PC, *i.e.*, at concentrations of a few vol %, does not produce the same protection against graphite exfoliation as does VC. The difference would appear to be due to the unique morphology and/or microstructure of the reduction layer formed by VC reduction.

*In situ* AFM measurements were carried out to investigate the electrode surface morphology during the electrochemical reduction of the 1% VC in THF, 0.1  $\text{LiClO}_4$  electrolyte at a GC electrode. Figure 4A shows a typical image of a freshly prepared GC electrode held at open circuit potential (OCP) *ca.* 2.0 V. The image displays a fairly uniform carbon surface with the average roughness of  $\sim 3.27$  nm. The randomly scattered shallow scratches and point defects on the surface were produced during the polishing process. The electrode potential was gradually decreased at 100 mV intervals from the initial OCP (2.0 V) to 0.8 V. A series of AFM images were recorded at each potential step. The AFM pictures were analyzed to find a correlation between the surface morphology and the CV characteristic. Visual examination of the AFM images reveals the presence of a surface film at 1.2 V (Fig. 4B), which becomes fully formed at 0.8 V (Fig. 4C). The film consists of tightly packed grains of  $\sim 50$  nm distributed uniformly over most of the surface except for a few deeper scratch marks.

To determine the thickness of the surface film after polarization at 0.8 V, we used the experimental procedure which was used by Siegenthaler and co-workers<sup>11</sup> to study the SEI films on highly ordered pyrolytic graphite. A  $1 \times 1 \mu\text{m}$  area of the electrode surface was selected and the SEI film was removed by abrasive etching, *i.e.*, repeated scanning of the AFM tip at high tip-to-sample force till no change of the surface morphology could be further induced. Following the abrasive etching, the electrode surface was scanned over a larger  $5 \times 5 \mu\text{m}$  area to image a cavity created in the SEI layer. Figure 5 shows the electrode morphology image with a square cavity in the center of the image and the corresponding height profile across the modified area. The thickness of the SEI film determined from the height profile was estimated to be *ca.*  $12 (\pm 3)$  nm.

To provide more insight into SEI film formation, a statistical analysis of the AFM images was conducted. Average roughness of a  $2 \times 2 \mu\text{m}$  area from the same location at the electrode surface was

calculated and expressed as a function of electrode potential (Fig. 6). It should be noted that the time spent in each potential interval to acquire the AFM image (*ca.* 2 min) is greater than the time elapsed in the same interval in CV (*ca.* 40-100 s) by about a factor of 2-3. The root mean square roughness decreased from 3.25 to 3.08 nm after a potential step from 1.8 to 1.5 V, and then increased slightly after steps to 1.4 and 1.2 V. Further decrease to 0.8 V combined with prolonged polarization produced substantial changes in electrode morphology and led to a significant increase of surface roughness to 3.65 nm. The initial drop of surface roughness at potentials below 1.8 V is consistent with formation of a thin film which predominantly fills in small cavities and scratches on the surface, *i.e.*, smoothing it out. This layer could be a result of precipitation of  $\text{LiOH}$ , a product from water reduction which starts at 1.8 V. As the reduction of VC takes place below 1.4 V, a surface layer with a different morphology begins to develop resulting in an increased

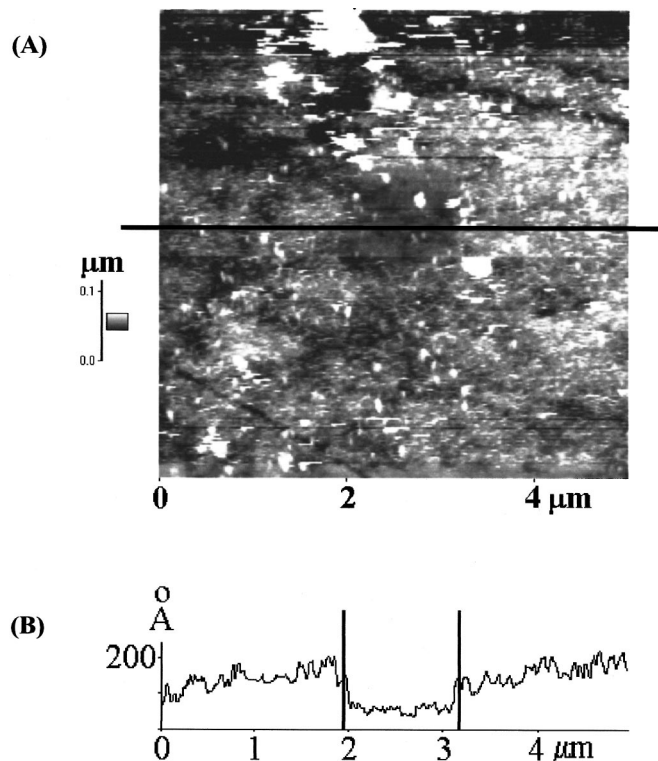
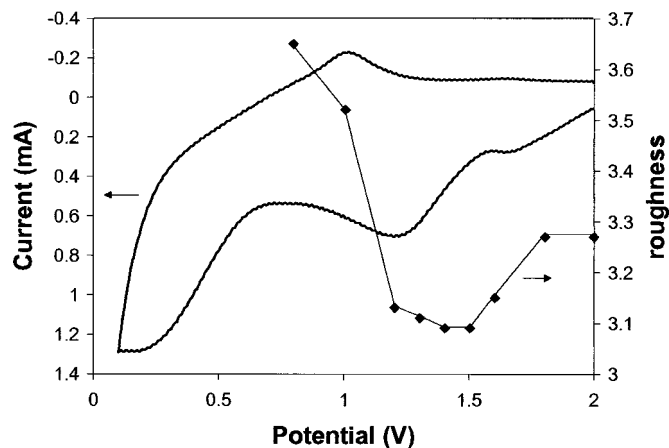


Figure 5. AFM image and depth profile of electrode surface after reduction at 0.8 V. An area of size  $2 \times 2 \mu\text{m}$  in the center was scratched off by increasing the force of AFM tip (see text).



**Figure 6.** Correlation of the voltammetry and the AFM determined roughness (nm) of the electrode surface at selected potentials for 1 vol % VC in THF-LiClO<sub>4</sub> electrolyte.

surface average roughness. The IRRAS results discussed earlier in the paper suggest this is the formation of lithium vinyl carbonate salt.

### Conclusions

The electrochemical reduction of five organic carbonates, EC, PC, DEC, DMC, and VC were studied via cyclic voltammetry at a Au electrode. More detailed studies of the chemistry of VC reduction were carried out using IRRAS at a GC electrode. The measured reduction potentials for EC, DEC, and PC were consistent with thermodynamic values calculated using density functional theory assuming one-electron reduction to the radical anion as the first step. The experimental values for VC and DMC were, however, much more positive than the calculated values, which we attribute to different reaction pathways. The role of VC as an additive in a PC-based electrolyte was investigated. We confirmed stable cycling of a

commercial li-ion battery carbon anode in a PC-based electrolyte with 5 mol % VC added. A surface layer indicative of preferential reduction of VC in the PC-based electrolyte was observed by IRRAS. The *in situ* electrochemical AFM study provided a clear evidence of the SEI layer formation on the GC electrode in the 1% VC in THF/0.1 M LiClO<sub>4</sub> electrolyte when the potential was stepped down to 0.8 V. The preferential reduction of VC and the SEI layer formation therefrom appears to inhibit PC cointercalation and subsequent graphite exfoliation.

### Acknowledgments

This research was funded by the Assistant Secretary for Energy Efficiency and Renewable Energy, Office of Advanced Automotive Technologies, U.S. Department of Energy, under contract DE-AC03-76SF00098. We thank Hans Siegenthaler for a copy of their paper prior to publication.

*The University of California assisted in meeting the publications costs of this article.*

### References

1. A. N. Dey and B. P. Sullivan, *J. Electrochem. Soc.*, **117**, 222 (1970).
2. M. Winter, J. O. Besenhard, M. E. Spahr, and P. Novak, *Adv. Mater.*, **10**, 725 (1998).
3. C. Wang, H. Nakamura, H. Komatsu, M. Yoshio, and H. Yoshitake, *J. Power Sources*, **74**, 142 (1998).
4. C. Jehoulet, P. Biensan, J. M. Bodet, M. Broussely, C. Moteau, and C. Tessier-Lescouret, Abstract 135, p. 153, The Electrochemical Society and International Society of Electrochemistry Meeting Abstracts, Vol. 97-2, Paris, France, Aug 31-Sept 5 (1997).
5. X. Zhang, J. K. Pugh, and P. N. Ross, Abstract 179, The Electrochemical Society Meeting Abstracts, Vol. 2000-2, Phoenix, AZ, Oct 22-27, 2000.
6. P. Andricacos and P. Ross, *J. Electrochem. Soc.*, **130**, 1355 (1983).
7. D. Aurbach, M. Daroux, P. Faguy, and E. Yeager, *J. Electroanal. Chem.*, **297**, 225 (1991).
8. S. A. Campbell, C. Bowes, and R. S. McMillan, *J. Electroanal. Chem.*, **284**, 195 (1990).
9. D. Pletcher, J. F. Rohan, and A. G. Ritchie, *Electrochim. Acta*, **39**, 1369 (1994).
10. B. Smith, *Infrared Spectral Interpretation*, CRC Press LLC, Boca Raton, FL (1998).
11. D. Alliata, R. Kötz, P. Novák, and H. Siegenthaler, *Electrochem. Commun.*, In press.